Porosity and thermal collapse measurements of H_2O, CH_3OH, CO_2, and H_2O:CO_2 ices

K. Isokoski, J.-B. Bossa, T. Triemstra and H. Linnartz

Raymond and Beverly Sackler Laboratory for Astrophysics, Leiden Observatory, Leiden University, Netherlands

Phys.Chem.Chem.Phys., 2014, 16, 3456

By

Rabin Rajan J M

24-05-2014

Introduction

- Amorphous solid water (ASW), CO_2, CH_3OH are amoung the major component of interstellar and cometary ices.
- The ice mixture structure and its effect on chemical reactivity are less understood.
- Agreement exists about the fact that the ices in space are typically amorphous, but the amount of porosity is still under debate.
- Porous ices provide large and effective surface area for adsorption of atoms and molecules, catalysis of chemical reactions and further retention of the involved species.

Porosity in interstellar ices ?????

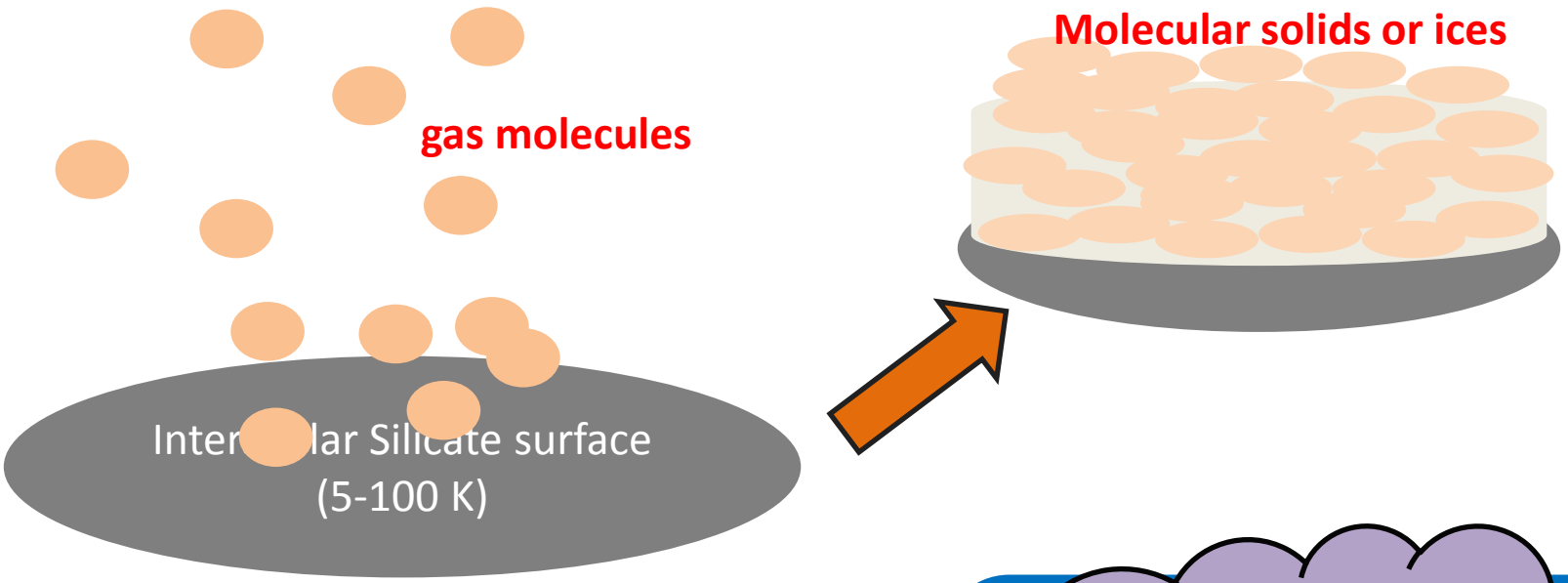

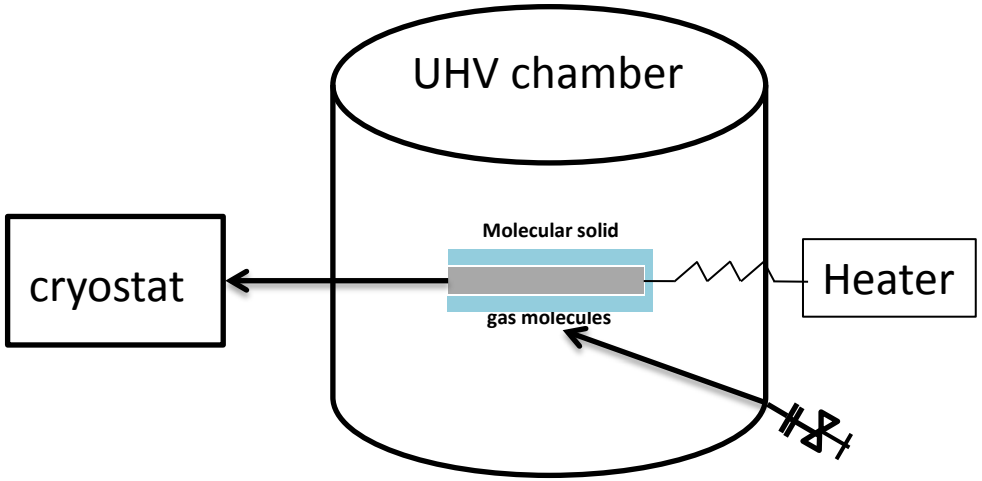

How this is experimentally studied ????

Introduction (continued…)

What porosity can lead to???

- Large quantities of molecules can be stored inside pores and later can be thermally released.
- The porous to compact transition or a structural collapse at low temperatures can enhance the limited recombination of reactive species normally trapped in such ice matrix.

In this paper

- Quantitative determination of ice porosity and thermal collapse upon heating is measured using laser optical interference and Infrared spectroscopy for H_2O, CH_3OH, CO_2 and H_2O:CO_2= 2:1 ices

Experimental approach

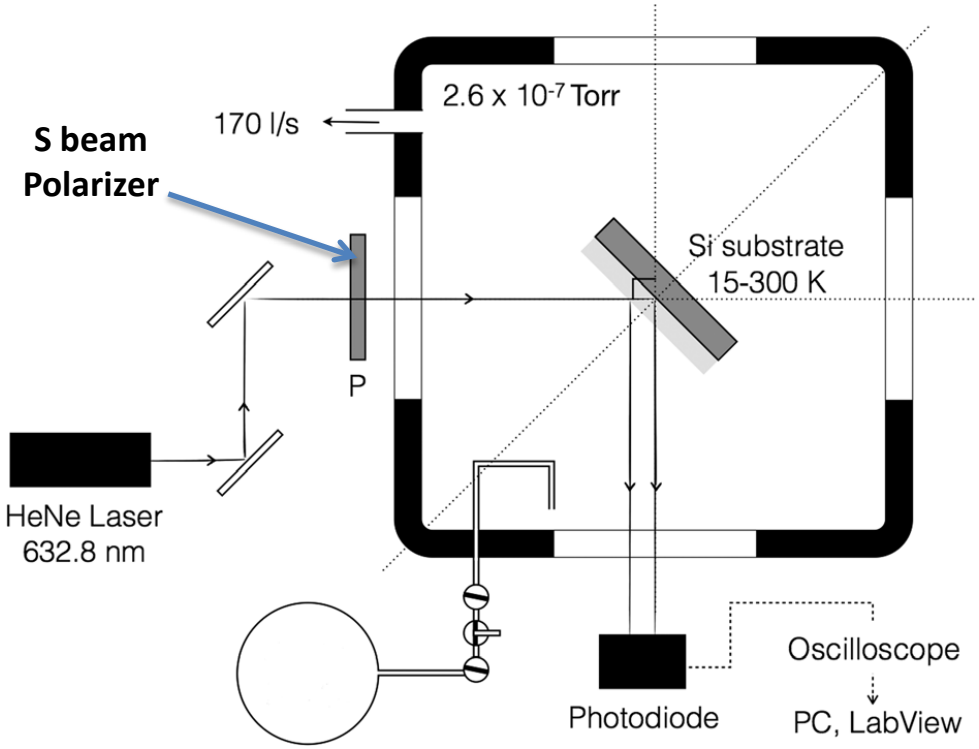

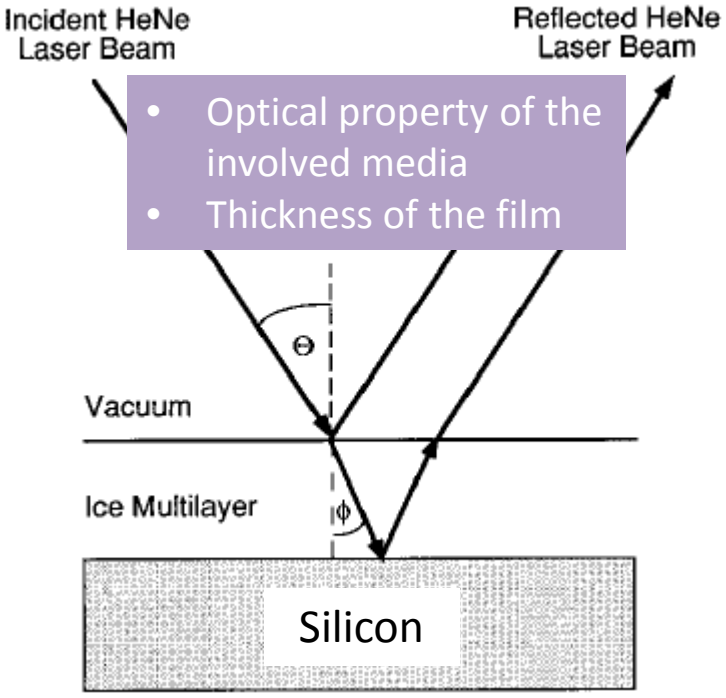

- Optical property of the involved media
- Thickness of the film

Fig. 1 Schematic drawing of the experimental setup used to measure thin-film interference in pure H_2O and CH_3OH ices. P = linear polarizer.

Measurable photo diode signal S (in volts) is related to $|R|^2$ through an empirical factor, α intrinsic to photodiode

Refractive index of ice at a particular temperature is constant

$$R = \frac{r_{01} + r_{12}e^{-i2\beta}}{1 + r_{01}r_{12}e^{-i2\beta}}, \qquad r_{01s}$$

$$\beta = \frac{2\pi d}{\lambda} \times n_1 \cos\theta_1, \qquad r_{12s}$$

$\times\ t$

r_{01} and r_{02} are Fresnel reflection coefficients of the interfaces, d thickness of ice, n_1 refractive index of ice, n_o refractive index of vacuum and n_2 refractive index of silicon substrate. Incident angles θ_0 and θ_1 are related through Snells law (n_0 si

t and γ deposition time and rate

Results and discussions

Deposition

$$S(n_1, \alpha, \gamma) = \alpha \times \left| \frac{r_{01}(n_1) + r_{12}(n_1)e^{-i2\beta(n_1,d)}}{1 + r_{01}(n_1)r_{12}(n_1)e^{-i2\beta(n_1,d)}} \right|^2 \qquad d = \gamma \times t$$

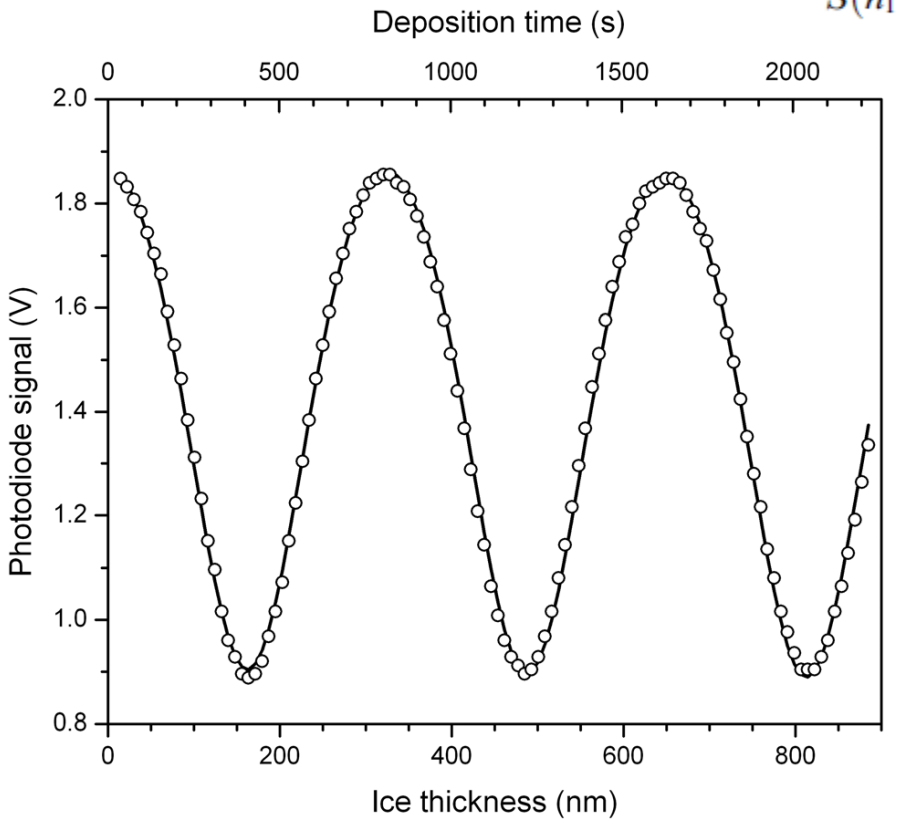

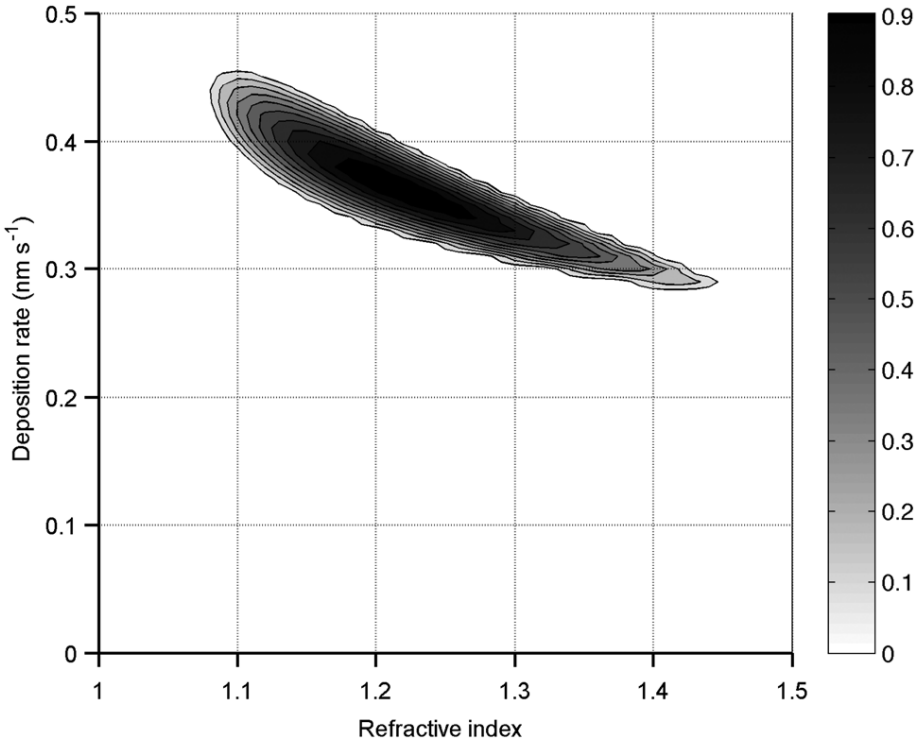

Fig. 2 Optical interference signal during deposition of a pure H_2O ice sample at 20 K (reduced data points, open circles) and the best fit (solid line) using eqn (5). The first and last point indicate the start and the end of the deposition process, respectively.

Fig. 3 Coefficient of determination (R^2, color bar) from the fits using eqn (5) for a pure H2O ice sample deposited at 20 K as a function of the refractive index n_1, and the deposition rate γ, with the scaling factor α fixed to an optimised value.

Refractive indices and deposition rates

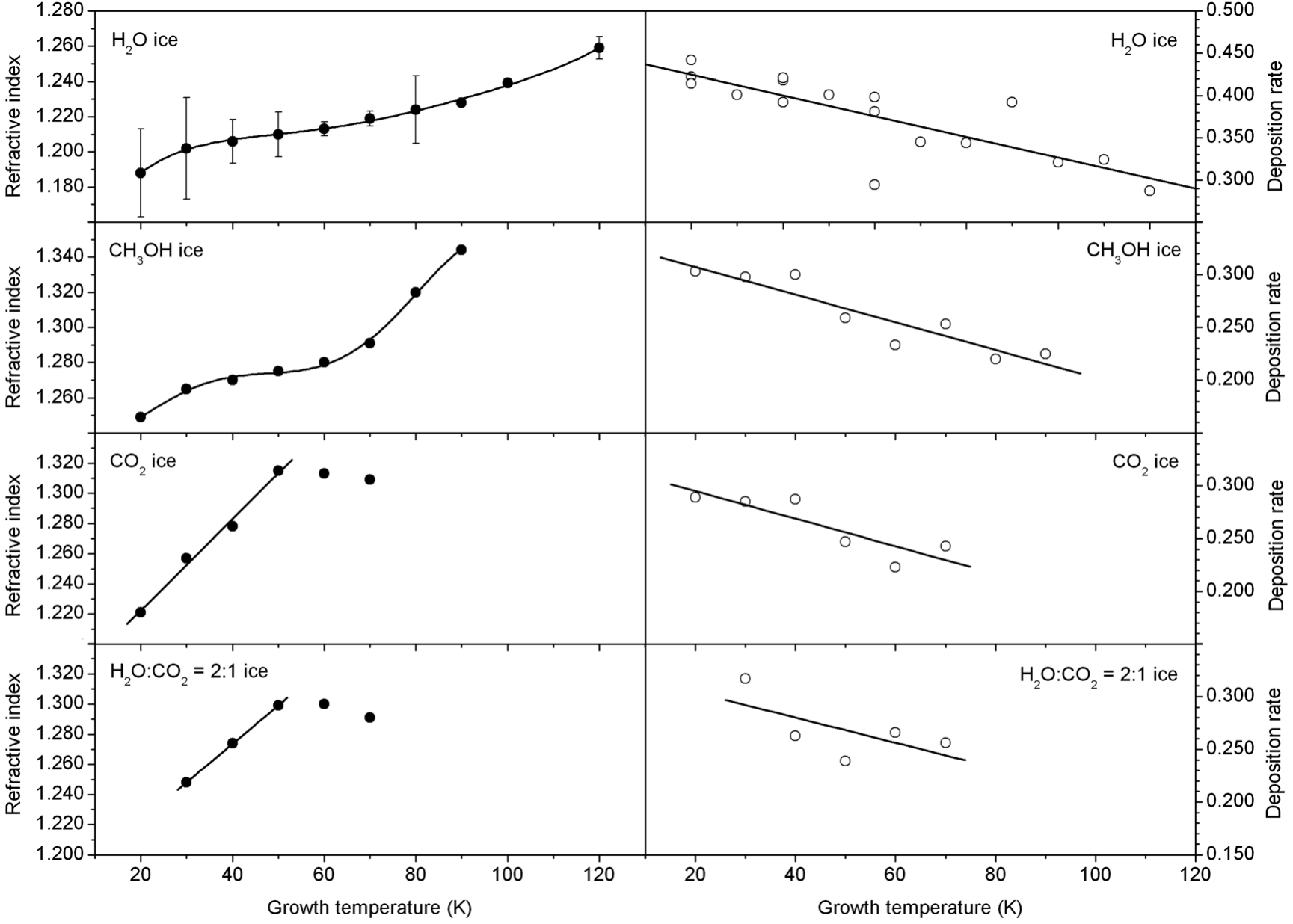

Fig. 4 Refractive indices (full circles) and deposition rates (open circles) obtained for H_2O, CH_3OH, CO_2 and H_2O:CO_2 = 2 : 1 ice samples as a function of the growth temperature. The polynomial and linear fits are shown as solid lines. The error bars (top left panel) are representative of the repeatability of the procedure at the 95% confidence level.

Thermal annealing

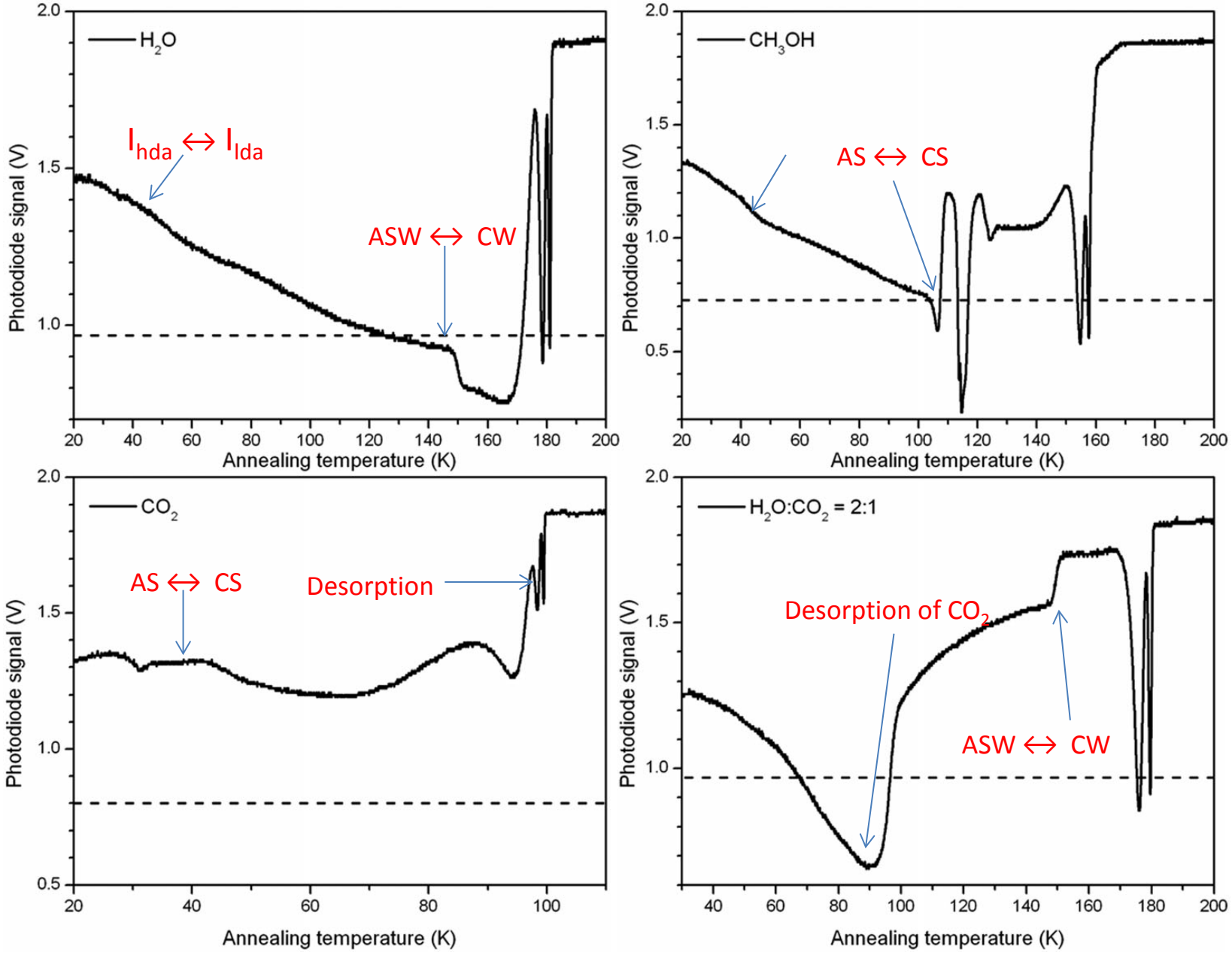

Fig. 5 Interference signal during thermal annealing or H_2O, CH_3OH, CO_2 and H_2O:CO_2 = 2 : 1 ice samples. The dashed line indicates the lowest signal obtained during the initial deposition.

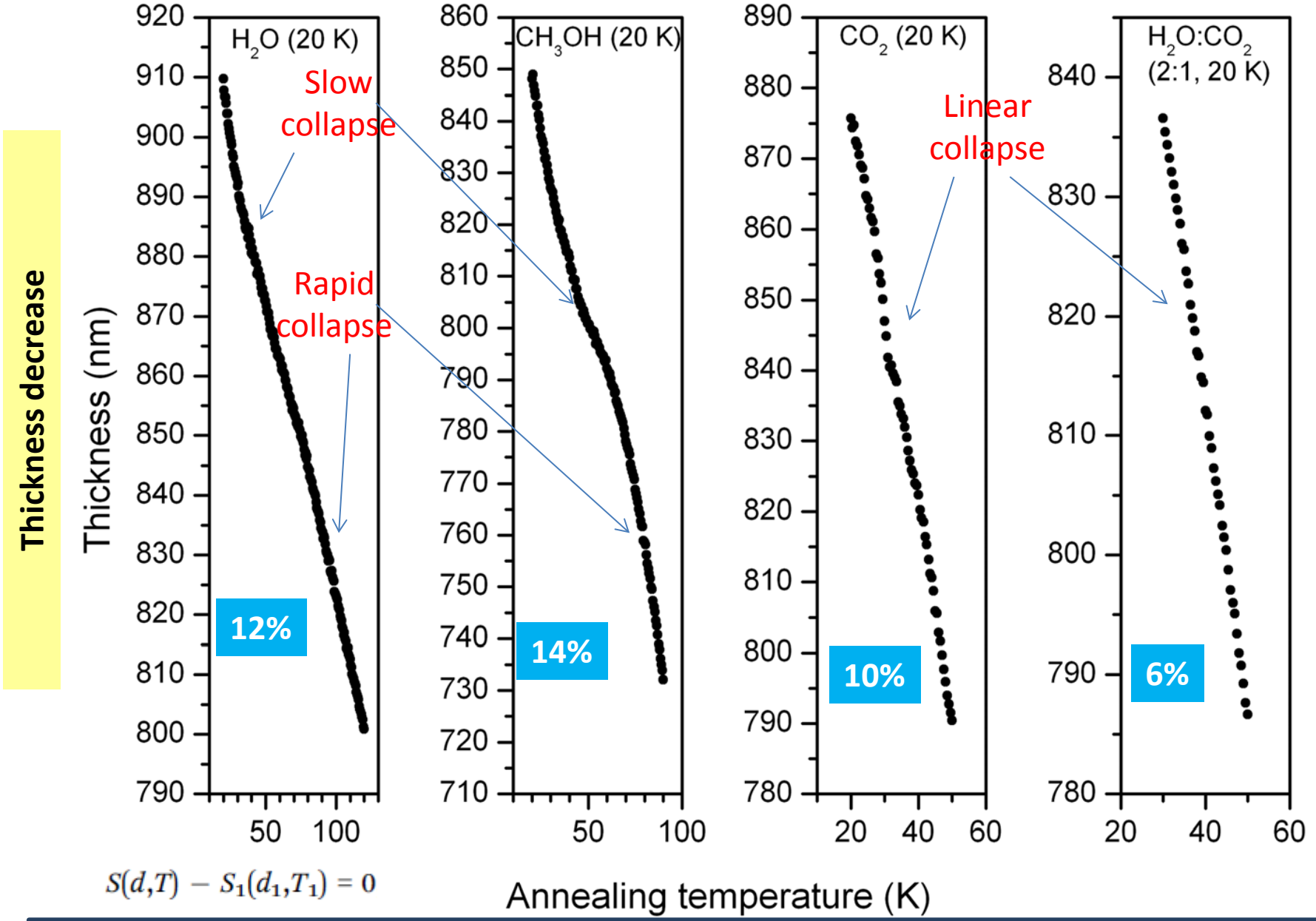

Fig. 6 Thickness decrease upon thermal annealing of H_2O, CH_3OH, CO_2 ice deposited at 20 K and H_2O:CO_2 = 2 : 1 ice deposited at 30 K. Note that the thickness and temperature ranges are not equal.

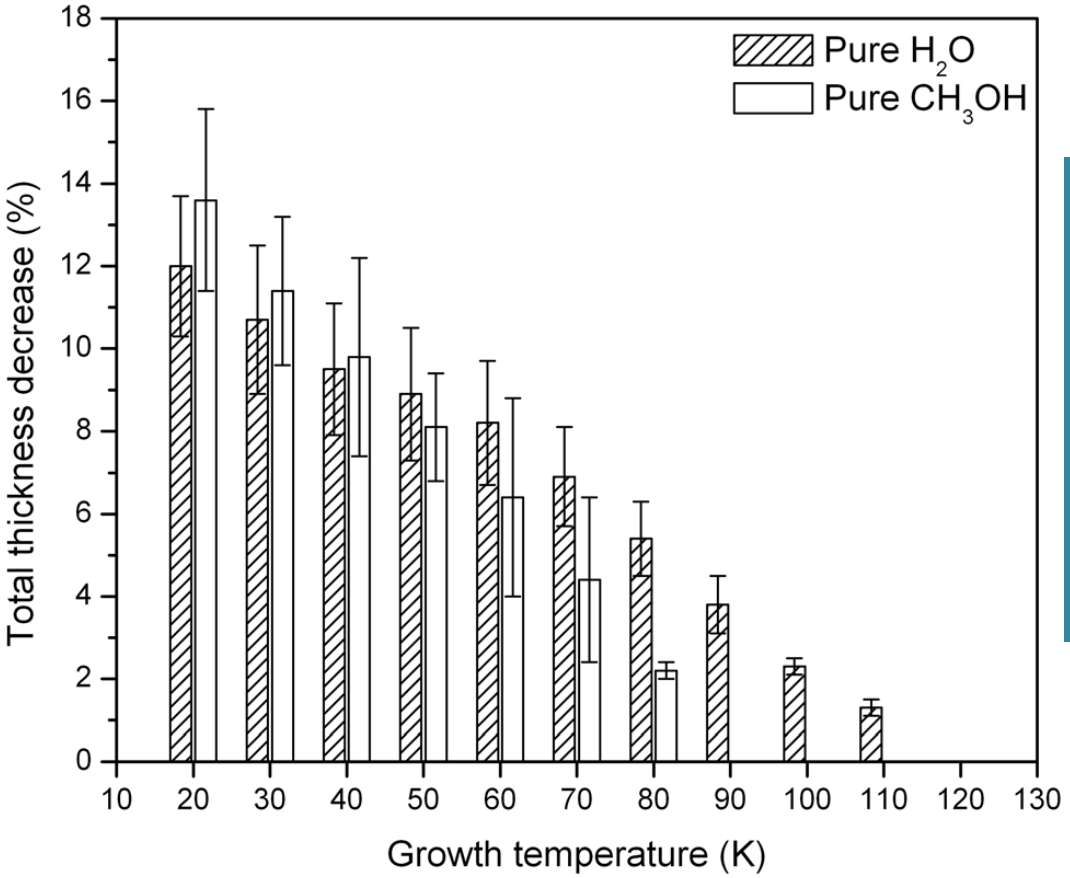

- The total structural collapse decreases linearly with the growth temperature.
- Extrapolating these data, shows that ices grown near their crystallisation temperature are compact and the total thickness decrease or equals zero.

Fig. 7 Total thickness decrease (in %) of pure H_2O and CH_3OH ice samples deposited at different growth temperatures and then thermally annealed to 120 K and 90 K, respectively.

Residual porosity in annealed H_2O

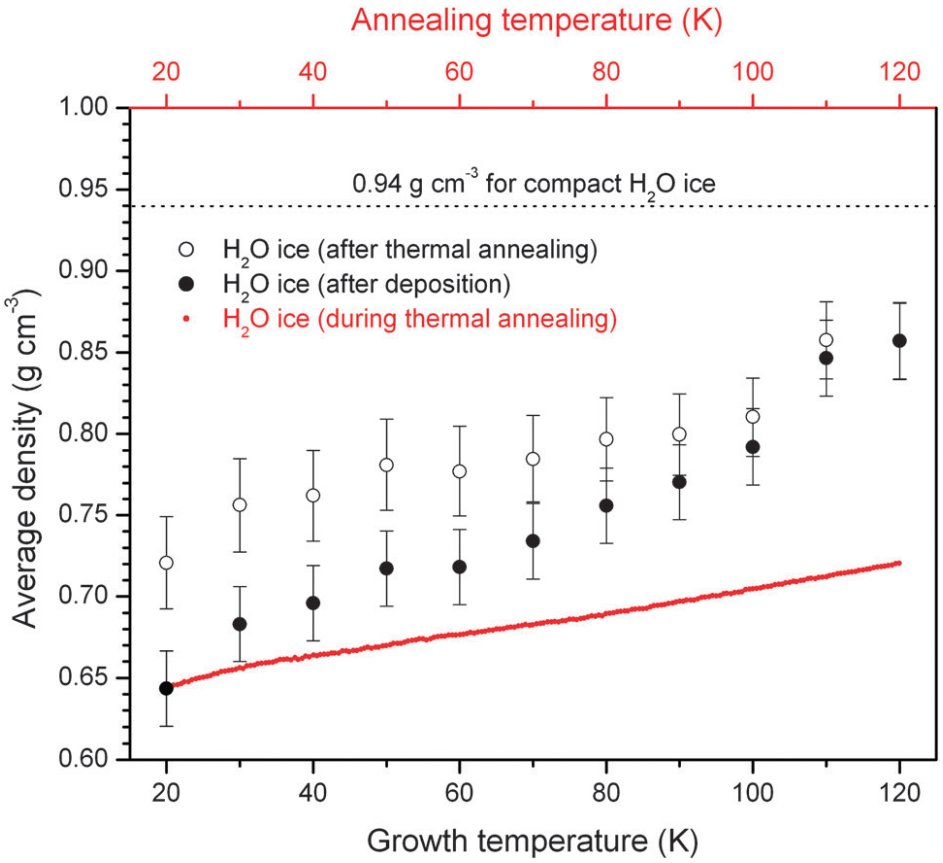

From the Lorentz–Lorenz equation, we can relate each measured refractive index n_1 to the initial porosity p and the initial density ρ,

$$p = 1 - \left(\frac{{n_1}^2 - 1}{{n_1}^2 + 2} \times \frac{n_i^2 + 2}{n_i^2 - 1} \right) = 1 - \frac{\rho}{\rho_c}$$

n_i = 1.285, ρ_c = 0.94 g cm^3 the intrinsic refractive index and density of H_2O ice (i.e., not including pores)

Fig. 8 Average density of porous H_2O ice samples after deposition (black circles) and after thermal annealing to 120 K (open circles). Black and open circles for one specific temperature show the start and end point during an annealing experiment, respectively. This is illustrated by the red line for one selected measurement of a porous H_2O ice sample grown at 20 K and heated with 2 K min^{-1}, showing the average density as a function of the annealing temperature (upper x-axis).

- **Residual porosity is observed.**
- **Original approximation is valued to longer time scales.**
- **The values in Fig 7 should be considered as upper limits**

Segregation of CO_2 in annealed H_2O: CO_2 (2:1) ice

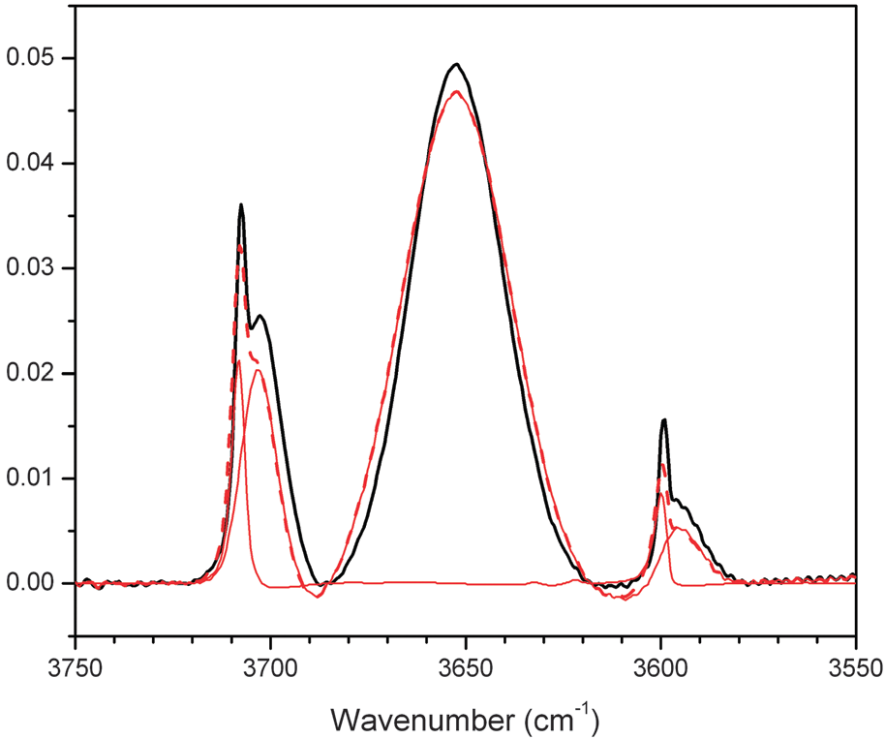

Fig. 9 Example of an infrared spectrum of $H_2O:CO_2$ = 2 : 1 deposited at 20 K then warmed up to 70 K (black line), fitted with a porous CO_2 ice spectrum and a porous $H_2O:CO_2$ ice spectrum background deposited at 40 K (red solid lines). The combined fit is the red dashed line.

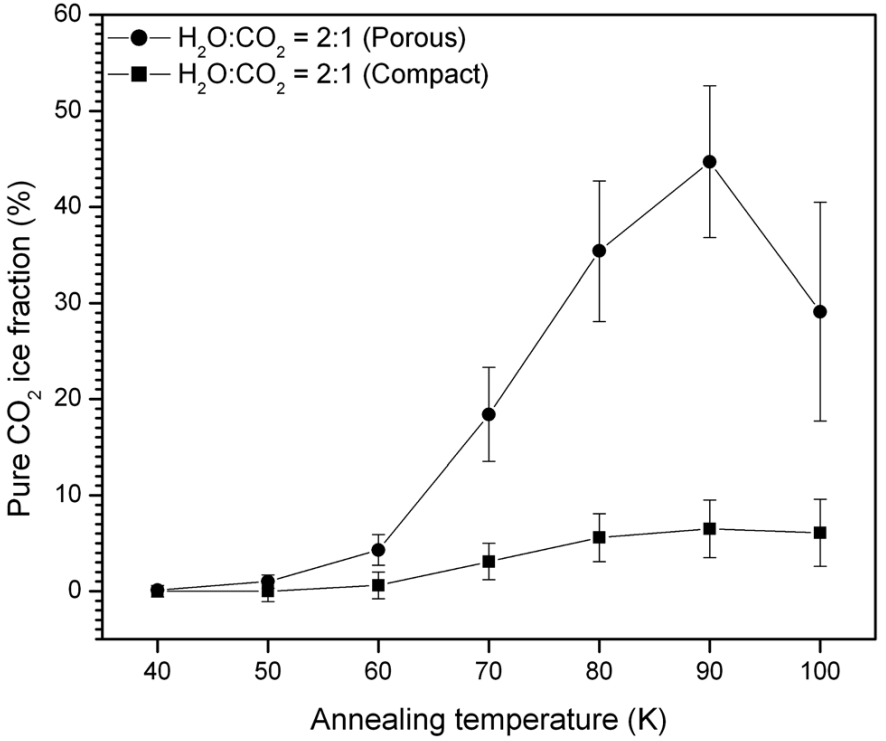

Fig. 10 Pure CO_2 ice fraction (in percent) in the $H_2O:CO_2$ = 2 : 1 ice sample upon thermal annealing for porous ice (circles) and compact ice (squares).

More porosity leads to more segregation . The pure CO_2 ice fraction reaches about 45% at 90 K for an initial porous ice in contrast to about 6.5% for an initial compact ice at the same temperature.

Summary and conclusions

- ✓ The thickness decrease of H_2O, CH_3OH, CO_2 and H_2O:CO_2= 2:1 ice samples upon thermal annealing in an astronomically relevant temperature range using laser optical interference together with FTIR spectroscopy was studied and they found the following

1) *Porous H_2O ice undergoes a gradual thermal collapse throughout the amorphous regime. A total thinning of about 12% is derived between 20 and 120 K. This value is an upper limit.*
2) *Porous H_2O ice is not fully compacted during the thermal annealing experiment time scale. Depending on the growth temperature, the residual porosity after annealing to 120 K can reach 17±3%.*

Summary and conclusions (continued…)

Large cavities remain in the ice throughout the solid phase, not observable though infrared spectroscopy of dangling OH bonds.

3) *The initial porosity of the ice determines its structure throughout the solid phase until ice evaporation. H_2O rich ices formed by vapour deposition on cold interstellar dust grains may contain large cavities that persist over a large temperature range, and affect the catalytic potential of the ice as well as the trapping of gases.*

4) *A high initial porosity leads to a higher extent of CO_2 segregation.*

Implication

- Thermal collapse on our porosity measurement study need to be looked upon. May be residual porosity is what we are able to measure.

- Initial porosity can be measured only when the molecule diffuse into the system at lower temperature.

- Segregation, phase separation near to desorption is observed in acetonitrile-water system can be explained in terms of porosity of water ice.

- Porosity driven reactions can be studied.


Thank You!